Eur. Phys. J. B **36**, 335–348 (2003)
DOI: 10.1140/epjb/e2003-00352-7

THE EUROPEAN PHYSICAL JOURNAL B

Self-energy-functional approach: Analytical results and the Mott-Hubbard transition

M. Potthoff[a]

Institut für Theoretische Physik und Astrophysik, Universität Würzburg, Germany

Received 12 June 2003 / Received in final form 3 November 2003
Published online 23 December 2003 –

Abstract. The self-energy-functional approach proposed recently is applied to the single-band Hubbard model at half-filling to study the Mott-Hubbard metal-insulator transition within the most simple but non-trivial approximation. This leads to a mean-field approach which is interesting conceptually: Trial self-energies from a two-site single-impurity Anderson model are used to evaluate an exact and general variational principle. While this restriction of the domain of the functional represents a strong approximation, the approach is still thermodynamically consistent by construction and represents a conceptual improvement of the "linearized DMFT" which has been suggested previously as a handy approach to study the critical regime close to the transition. It turns out that the two-site approximation is able to reproduce the complete (zero and finite-temperature) phase diagram for the Mott transition. For the critical point at $T = 0$, the entire calculation can be done analytically. This calculation elucidates different general aspects of the self-energy-functional theory. Furthermore, it is shown how to deal with a number of technical difficulties which appear when the self-energy functional is evaluated in practice.

PACS. 71.10.-w Theories and models of many-electron systems – 71.15.-m Methods of electronic structure calculations – 71.30.+h Metal-insulator transitions and other electronic transitions

1 Introduction

The correlation-driven transition from a paramagnetic metal to a paramagnetic insulator (Mott-Hubbard transition [1–3]) is one of the most interesting problems in condensed-matter physics. As a prime example for a quantum-phase transition, the Mott-Hubbard transition is important from the physical point of view but also for the development and test of general theoretical methods to treat correlated electron systems. The minimum model required to study the Mott-Hubbard transition is the single-band Hubbard model [4–6]. Inherent to this model is the competition between the electrons' kinetic energy which tends to delocalize the electrons and favors a metallic state and the on-site Coulomb interaction which tends to localize the electrons to avoid double occupancies and thereby favors an insulating state at half filling. Except for the one-dimensional case [7], however, exact results with regard to the nature of the transition and the critical interaction strength U_c are not available – even for this highly simplified model system. A direct numerical solution using exact-diagonalization or quantum Monte-Carlo methods [8] suffers from the difficulty to access the thermodynamic limit or the low-temperature, low-energy regimes.

Considerable progress has been made in recent years due to the development of the dynamical mean-field theory (DMFT) [9–11] which focuses on the opposite limit of infinite spatial dimensions $D = \infty$ [12–15]. Within the DMFT the problem is simplified by mapping the original lattice model onto an impurity model the parameters of which must be determined by a self-consistency condition. Different techniques to solve the effective impurity model have been employed to study the Mott transition within the DMFT, iterative perturbation theory [9,16,17], exact diagonalization [18–21], renormalization-group methods [22–24], and quantum Monte-Carlo [25–29]. One of the most important characteristic of the transition is the value of the critical interaction strength U_c at zero temperature. Roughly, the different techniques to solve the mean-field equations predict $U_c/W \approx 1 - 1.5$ where W is the width of the free density of states.

Recently, a self-energy-functional approach (SFA) has been put forward [30]. The SFA is a general variational approach to correlated lattice models where the grand potential Ω is considered as a functional of the self-energy $\boldsymbol{\Sigma}$. As this functional is constructed from an infinite series of renormalized skeleton diagrams, it is not known in an explicit form and the variational principle $\delta\Omega[\boldsymbol{\Sigma}] = 0$ cannot be exploited *directly*. Usually, one replaces the exact but unknown functional with an explicitly known but approximate one – this is essentially the standard diagrammatic

[a] e-mail: potthoff@physik.uni-wuerzburg.de

approach [7] which leads to weak-coupling approximations in the end [31]. Opposed to this weak-coupling perturbational approach, the functional dependence $\Omega[\boldsymbol{\Sigma}]$ is not approximated at all in the SFA. The key observation is that the functional, though unknown explicitly, can be evaluated on a restricted domain of trial self-energies $\mathcal{S}$. The evaluation of the functional is exact, while the approximation is due to the fact that the self-energy in the variational principle is no longer considered as arbitrary. In this way, depending on the choice for the space $\mathcal{S}$, some well-known but also some novel approximations can be realized. Here we are interested in the single-band Hubbard model with Hamiltonian H. As argued in reference [30] a useful trial self-energy has to be constructed as the exact self-energy of a different model ("reference system") with Hamiltonian H'. The reference system can be chosen arbitrarily – it must, however, share the same interaction part with the original model H. The variational parameters at one's disposal are therefore the one-particle parameters of the reference system $\boldsymbol{t}'$. The trial self-energy is parameterized as $\boldsymbol{\Sigma} = \boldsymbol{\Sigma}(\boldsymbol{t}')$, and the variational principle reads $\partial\Omega[\boldsymbol{\Sigma}(\boldsymbol{t}')]/\partial\boldsymbol{t}' = 0$. To provide trial self-energies is the only purpose of the reference system H'. Whenever one is able to compute $\boldsymbol{\Sigma}$ for the reference system H', an exact evaluation of $\Omega[\boldsymbol{\Sigma}(\boldsymbol{t}')]$ is possible.

Choosing H' to be a system of decoupled sites, yields a Hubbard-I-type approximation. An improved approximation is obtained when H' consists of decoupled clusters with a finite number of sites $N_\mathrm{c} > 1$ per cluster as has been considered in references [32,33]. This approach not only recovers the so-called cluster-perturbation theory (CPT) [34–36] but also gives a variational improvement (V-CPT) which e.g. allows to describe phases with spontaneously broken symmetry [33]. Another possibility is to take $N_\mathrm{c} = 1$, which implies the trial self-energy to be local, but to include a coupling to a number of n_b additional uncorrelated ("bath") sites. In this case the reference system consists of a decoupled set of single-impurity Anderson models (SIAM) with $n_\mathrm{s} = 1 + n_\mathrm{b}$ sites each. As has been shown in reference [30], this approach not only recovers the DMFT (namely in the limit $n_\mathrm{b} \to \infty$) but also provides a new variant of the exact-diagonalization approach, namely for any finite n_b. As compared to previous DMFT-exact-diagonalization approaches [18–21], the construction gives a thermodynamically consistent approximation even for small n_b. More complicated reference systems may be taken for the construction of consistent approximations, for example a system of decoupled clusters of size N_c where each site in the cluster is coupled to n_b additional bath sites. It has been shown [32] that in the limit $n_\mathrm{b} \to \infty$ the cellular DMFT (C-DMFT) is obtained [37], while approximations with finite n_b represent cluster approximations which "interpolate" between the CPT ($n_\mathrm{b} = 0$) and the C-DMFT ($n_\mathrm{b} = \infty$).

In the present paper the Mott transition is studied within the most simple but non-trivial approximation: The variational principle $\delta\Omega[\boldsymbol{\Sigma}] = 0$ is exploited using a local trial self-energy from a reference system with $N_\mathrm{c} = 1$ and a single additional bath site only, $n_\mathrm{b} = 1$. As $n_\mathrm{s} = 1 + n_\mathrm{b} = 2$ this approximation will be referred to as the two-site dynamical impurity approximation ($n_\mathrm{s} = 2$-DIA) in the following.

The paper is organized as follows: A brief review of the self-energy-functional approach will be given in the next Section 2. The general aspects of the evaluation of the SFA are discussed in Section 3 while Section 4 focuses on local approximations ($N_\mathrm{c} = 1$, n_s arbitrary) in particular. In Section 5 the further specialization to the case $n_\mathrm{s} = 2$ is considered. The $n_\mathrm{s} = 2$ dynamical-impurity approximation is motivated (i) by the fact that at the critical point for the Mott transition the entire calculation can be done *analytically*, (ii) by the conceptual simplicity of the approach which rests on a *single* approximation only and (iii) by making contact with a linearized DMFT (L-DMFT) [38–43] developed previously. This is discussed in detail in Section 5 while Section 6 then presents the analytical calculation for the critical regime. The results are discussed in Section 7. The complete phase diagram for $T = 0$ and finite temperatures is addressed in Section 8 and the conclusions are given in Section 9.

2 Self-energy-functional theory

Useful information on correlated electron systems can be gained by exact-diagonalization or quantum Monte-Carlo methods applied to a lattice of finite size [8]. This approach, however, suffers from the difficulty to access the thermodynamic limit and is therefore of limited use to describe phases with long-order and phase transitions. On the other hand, using an *embedding approximation*, one can directly work in the thermodynamic limit and describe phase transitions while the actual numerical treatment has to be done a system of finite size only. In the context of an embedding technique we have to distinguish between the original model of infinite size H and an (e.g. spatially) truncated *reference system* H'. The reference system must not necessarily be finite but it may consist of an infinite number of decoupled subsystems with a finite number of degrees of freedom each. In any case, H' must be exactly solvable.

If one is interested not only in the equilibrium thermodynamics but also in the elementary one-particle excitations, an embedding technique should focus on a dynamical quantity, such as the frequency-dependent self-energy $\boldsymbol{\Sigma}$. The knowledge of $\boldsymbol{\Sigma}$ then allows to derive a thermodynamic potential Ω as well as different static and dynamic quantities via general relations. The main steps are the following: (i) Truncate the original model H to obtain a simpler model H' which is tractable numerically. (ii) Calculate the self-energy $\boldsymbol{\Sigma}'$ of the reference system. (iii) Use $\boldsymbol{\Sigma} = \boldsymbol{\Sigma}'$ as an approximation for the self-energy of H and determine the grand potential Ω as well as further quantities of interest. (iv) To get a self-consistent scheme, optimize the parameters of H' by a feedback from the approximate solution at hand. Ideally, the last step should be based on a general variational principle. This is exactly the strategy of the self-energy-functional approach (SFA) proposed recently [30]. A brief review of the essentials of this approach is given in the following.

Consider a system of fermions on an infinite lattice with on-site Coulomb interaction at temperature T and chemical potential μ. Its Hamiltonian $H = H_0(\boldsymbol{t}) + H_1(\boldsymbol{U})$ consists of a one-particle part which depends on a set of hopping parameters $\boldsymbol{t}$ and an interaction part with Coulomb-interaction parameters $\boldsymbol{U}$:

$$H = \sum_{\alpha\beta} t_{\alpha\beta} c_\alpha^\dagger c_\beta + \frac{1}{2} \sum_{\alpha\beta\gamma\delta} U_{\alpha\beta\delta\gamma} c_\alpha^\dagger c_\beta^\dagger c_\gamma c_\delta \,. \qquad (1)$$

The grand potential Ω can be obtained from the stationary point of a self-energy functional

$$\Omega_{\boldsymbol{t}}[\boldsymbol{\Sigma}] \equiv \mathrm{Tr} \ln \left(-(\boldsymbol{G}_0^{-1} - \boldsymbol{\Sigma})^{-1} \right) + F[\boldsymbol{\Sigma}] \qquad (2)$$

as has been discussed in reference [30]. Here the subscript $\boldsymbol{t}$ indicates the parametric dependence of the functional on the hopping. This dependence is *exclusively* due to $\boldsymbol{G}_0 = 1/(\omega + \mu - \boldsymbol{t})$, the free Green's function of H. Further, $F[\boldsymbol{\Sigma}]$ is the Legendre transform of the Luttinger-Ward functional $\Phi[\boldsymbol{G}]$. As the latter is constructed as an infinite series of renormalized skeleton diagrams [7], the self-energy functional is not known explicitely. Nevertheless, the *exact* evaluation of $\Omega_{\boldsymbol{t}}[\boldsymbol{\Sigma}]$ and the determination of the stationary point is possible [30] on a *restricted* space $\mathcal{S}$ of trial self-energies $\boldsymbol{\Sigma}(\boldsymbol{t}') \in \mathcal{S}$. Due to this restriction the procedure becomes an approximation.

Generally, the space $\mathcal{S}$ consists of $\boldsymbol{t}'$ representable self-energies. $\boldsymbol{\Sigma}$ is termed $\boldsymbol{t}'$ representable if there are hopping parameters $\boldsymbol{t}'$ such that $\boldsymbol{\Sigma} = \boldsymbol{\Sigma}(\boldsymbol{t}')$ is the exact self-energy of the model $H' = H_0(\boldsymbol{t}') + H_1(\boldsymbol{U})$ ("reference system"). Note that both the original system H and the reference system H' must share the same interaction part. For any $\boldsymbol{\Sigma}$ parameterized as $\boldsymbol{\Sigma}(\boldsymbol{t}')$ we then have [30]:

$$\begin{aligned} \Omega_{\boldsymbol{t}}[\boldsymbol{\Sigma}(\boldsymbol{t}')] = {} & \Omega'(\boldsymbol{t}') \\ & + \mathrm{Tr} \ln \left(-(\boldsymbol{G}_0(\boldsymbol{t})^{-1} - \boldsymbol{\Sigma}(\boldsymbol{t}'))^{-1} \right) \\ & - \mathrm{Tr} \ln \left(-(\boldsymbol{G}_0(\boldsymbol{t}')^{-1} - \boldsymbol{\Sigma}(\boldsymbol{t}'))^{-1} \right) \,, \end{aligned} \qquad (3)$$

where $\Omega'(\boldsymbol{t}')$, $\boldsymbol{G}_0' \equiv \boldsymbol{G}_0(\boldsymbol{t}') = 1/(\omega + \mu - \boldsymbol{t}')$, and $\boldsymbol{\Sigma}(\boldsymbol{t}')$ are the grand potential, the free Green's function and the self-energy of the reference system H' while $\boldsymbol{G}_0$ is the free Green's function of H. For a proper choice of $\boldsymbol{t}'$, a (numerically) exact computation of these quantities is possible. Hence, the self-energy functional (3) can be evaluated exactly for this $\boldsymbol{\Sigma} = \boldsymbol{\Sigma}(\boldsymbol{t}')$. A certain approximation is characterized by a choice for $\mathcal{S}$. As $\boldsymbol{\Sigma}$ is parameterized by $\boldsymbol{t}'$, this means to specify a space of variational parameters $\boldsymbol{t}'$. Any choice will lead by construction to a non-perturbative approach which is thermodynamically consistent as an explicit expression for a thermodynamical potential is provided. It turns out that a stationary point of the self-energy functional is a saddle point in general. As in different standard variational methods, such as in the time-dependent density-functional approach [44], in the Green's-function approach [31] and also in a recently considered variant [45], this implies that there is no strict upper bound for the grand potential. For a further discussion of the general concepts of the SFA see reference [30].

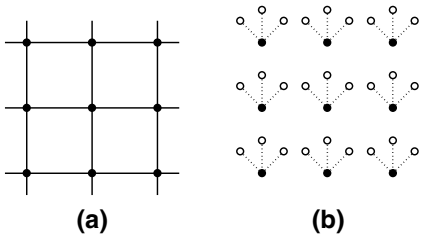

Fig. 1. Schematic representation of the single-band Hubbard model H (a) and a possible reference system H' (b). H' is a set of decoupled single-impurity Anderson models with one correlated ($U > 0$) impurity site and a number of $n_\mathrm{s} - 1$ uncorrelated ($U = 0$) bath sites each. In the figure $n_\mathrm{s} = 4$. Note that the interaction part is the same for (a) and (b). Variational parameters are the one-particle parameters of H'.

So far the discussion is completely general. In Section 4 we will consider H to be the Hubbard model and H' to be a system of decoupled single-impurity Anderson models (SIAM). Each SIAM consists of n_s sites, one correlated site (with $U > 0$) and $n_\mathrm{s} - 1$ uncorrelated "bath" sites ($U = 0$). This is illustrated by Figure 1 for $n_\mathrm{s} = 4$. Note that for any choice of n_s, the original system and the reference system share the same interaction part – as required by the general theory. The one-particle parameters of H' are the variational parameters, i.e. the one-particle energies of the original sites and the bath sites and the hopping ("hybridization") between them. As noted in reference [30], the dynamical mean-field theory (DMFT) is recovered in the limit $n_\mathrm{s} \to \infty$. For $n_\mathrm{s} < \infty$ one obtains a new variant of the DMFT-exact-diagonalization approach [18–21]. For a finite number of bath sites, the DMFT self-consistency condition cannot be strictly satisfied. In the DMFT-ED method one therefore has to introduce a certain measure which allows to minimize the error due to the discretization of the bath. The conceptual advantage of the SFA consists in the fact that this measure is replaced by a variational procedure which is based on a physical variational principle. As shown in reference [30], a very good quantitative agreement with results from full DMFT calculations can be achieved for the quasi-particle weight even with $n_\mathrm{s} = 4$. With $n_\mathrm{s} = 2$ a much simpler approach is considered here (Sects. 5 and 6) which, however, is still thermodynamically consistent and allows for simple and systematic investigations of the Mott transition.

3 Evaluation of the self-energy functional

The evaluation of the self-energy-functional theory can be done by solving the Euler equation [30] corresponding to the variational principle. While such an approach is possible in principle, it appears complicated as dynamical two-particle quantities of the reference system are required. An attractive alternative consists in the direct calculation of the grand potential along equation (3). The numerical computation of $\Omega_{\boldsymbol{t}}[\boldsymbol{\Sigma}(\boldsymbol{t}')]$ for a given set of one-particle parameters $\boldsymbol{t}'$ is straightforward for a reference system H' of finite size. There are, however, a few technical difficulties

which appear in the practical calculation and which shall be discussed in the following. The problem of finding a stationary point of the function $\boldsymbol{t}' \to \Omega_{\boldsymbol{t}}[\boldsymbol{\Sigma}(\boldsymbol{t}')]$ is not addressed here as this is a standard numerical problem very similar to the problem of finding a minimum of a real single-valued function of several arguments.

$\Omega_{\boldsymbol{t}}[\boldsymbol{\Sigma}(\boldsymbol{t}')]$ consists of three parts as given by equation (3). The grand potential of the reference system can be calculated as $\Omega'(\boldsymbol{t}') = -T \ln \mathrm{tr}' \exp(-(H' - \mu N')/T) = -T \ln \sum_m \exp(-(E'_m - \mu N'_m)/T)$ from the many-body eigenenergies $E'_m - \mu N'_m$ of $H' - \mu N'$ where N' is the total particle number operator. Direct numerical diagonalization or (at $T = 0$) the Lanczos technique [46] may be used.

Next, the second term on the r.h.s. of equation (3) is discussed. In the following the dependence of $\boldsymbol{\Sigma}$ on $\boldsymbol{t}'$ will be suppressed for convenience and its dependence on ω is made explicit in the notations. The diagonalization of $H' - \mu N'$ yields (via the Lehmann representation) the Green's function $\boldsymbol{G}'(\omega)$ and the free Green's function $\boldsymbol{G}'_0(\omega)$ of the reference system. The self-energy is then obtained from the Dyson equation of the reference system $\boldsymbol{\Sigma}(\omega) = {\boldsymbol{G}'_0}^{-1}(\omega) - {\boldsymbol{G}'}^{-1}(\omega)$. Using the self-energy $\boldsymbol{\Sigma}(\omega)$, one obtains the (approximate) Green's function of the original model via $\boldsymbol{G}(\omega) \equiv (\boldsymbol{G}_0^{-1}(\omega) - \boldsymbol{\Sigma}(\omega))^{-1}$. The remaining task is to calculate $\mathrm{Tr} \ln(-\boldsymbol{G})$ for a lattice consisting of a finite number of sites L. The thermodynamic limit $L \to \infty$ is performed in the end. Translational symmetry is not necessarily required.

It is important to note that $\boldsymbol{G}(\omega)$ is causal, i.e. $\boldsymbol{G}(\omega + i0^+) = \boldsymbol{G}_{\mathrm{R}}(\omega) - i\boldsymbol{G}_{\mathrm{I}}(\omega)$ with $\boldsymbol{G}_{\mathrm{R}}(\omega)$, $\boldsymbol{G}_{\mathrm{I}}(\omega)$ Hermitian and $\boldsymbol{G}_{\mathrm{I}}(\omega)$ positive definite for any real ω (0^+ is a positive infinitesimal). The causality of the Green's function $\boldsymbol{G}(\omega)$ is ensured by the causality of $\boldsymbol{\Sigma}(\omega)$ and $\boldsymbol{G}_0(\omega)$, see Appendix A. The latter are causal as these are exact quantities.

Let ω_m be the (real, first-order) poles of $\boldsymbol{G}(\omega)$. For $\omega \to \omega_m$ we have $\boldsymbol{G}(\omega) \to \boldsymbol{R}_m/(\omega - \omega_m)$ where due to the causality of $\boldsymbol{G}(\omega)$ the matrix $\boldsymbol{R}_m$ is positive definite. Therefore, the frequency-dependent diagonalization of $\boldsymbol{G}(\omega) = \boldsymbol{U}(\omega)\boldsymbol{g}(\omega)\boldsymbol{U}(\omega)^\dagger$ with unitary $\boldsymbol{U}(\omega)$ (for real ω) yields a diagonal Green's function $\boldsymbol{g}(\omega)$ with elements $g_k(\omega)$ that are real for real ω and have first-order poles at $\omega = \omega_m$ with *positive* residues.

As the Green's function can be written as $\boldsymbol{G}(\omega) = 1/(\omega + \mu - \boldsymbol{t} - \boldsymbol{\Sigma}(\omega))$, the unitary transformation $\boldsymbol{U}(\omega)$ also diagonalizes the real and symmetric matrix $\boldsymbol{t} + \boldsymbol{\Sigma}(\omega)$, i.e. $\boldsymbol{t} + \boldsymbol{\Sigma}(\omega) = \boldsymbol{U}(\omega)\boldsymbol{\eta}(\omega)\boldsymbol{U}(\omega)^\dagger$ and $g_k(\omega) = 1/(\omega + \mu - \eta_k(\omega))$. The $\eta_k(\omega)$ are real for real ω and have first-order poles at $\omega = \zeta_n$ with ζ_n being the poles of the self-energy. For $\omega \to \zeta_n$ we have $\boldsymbol{\Sigma}(\omega) \to \boldsymbol{S}_n/(\omega - \zeta_n)$ with positive definite $\boldsymbol{S}_n$. Consequently, the residues of $\eta_k(\omega)$ at $\omega = \zeta_n$ are *positive*.

One can write $g_k(\omega) = \sum_m R_{k,m}/(\omega - \omega_m) + \widetilde{g}_k(\omega)$ and $\eta_k(\omega) = \sum_n S_{k,n}/(\omega - \zeta_n) + \widetilde{\eta}_k(\omega)$ with $R_{k,m}, S_{k,n} > 0$ and where $\widetilde{g}_k(\omega)$ and $\widetilde{\eta}_k(\omega)$ are analytical in the entire ω plane. As $\boldsymbol{G}(\omega) \sim 1/\omega$ and $\boldsymbol{\Sigma}(\omega) \sim$ const. for $\omega \to \infty$, one has $\widetilde{g}_k(\omega) = 0$ and $\widetilde{\eta}_k(\omega) =$ const. and real. Consequently, $-(1/\pi)\mathrm{Im}\, g_k(\omega + i0^+) \geq 0$ and $-(1/\pi)\mathrm{Im}\, \eta_k(\omega + i0^+) \geq 0$. This will be used in the following.

The trace "Tr" in equation (3) consists of a sum $T \sum_\omega$ over the fermionic Matsubara frequencies $i\omega = i(2n+1)\pi T$ (n integer) and a trace "tr" with respect to the quantum numbers α; see equation (1). The convergence of the frequency sum is ensured by the usual factor $\exp(i\omega 0^+)$ from the diagram rules. The calculation then proceeds as follows:

$$
\begin{aligned}
& T \sum_\omega e^{i\omega 0^+} \mathrm{tr}\, \ln \frac{-1}{i\omega + \mu - \boldsymbol{t} - \boldsymbol{\Sigma}(i\omega)} \\
& \overset{\text{(a)}}{=} \frac{-1}{2\pi i} \sum_k \oint_C d\omega\, e^{\omega 0^+} f(\omega)\, \ln\left(-g_k(\omega)\right) \\
& \overset{\text{(b)}}{=} \frac{-1}{\pi} \sum_k \int_{-\infty}^{\infty} d\omega\, f(\omega)\, \mathrm{Im}\, \ln(-g_k(\omega + i0^+)) \\
& \overset{\text{(c)}}{=} -\sum_k \int_{-\infty}^{\infty} d\omega\, f(\omega)\, \Theta\left(\omega + \mu - \eta_k(\omega)\right) \\
& \overset{\text{(d)}}{=} -\sum_k \int_{-\infty}^{\infty} d\omega\, T\, \ln(1 + e^{-\omega/T}) \frac{d\Theta(\omega + \mu - \eta_k(\omega))}{d\omega} \\
& \overset{\text{(e)}}{=} -2L \sum_m T\, \ln(1 + \exp(-\omega_m/T)) - R_\Sigma
\end{aligned}
\tag{4}
$$

with

$$
R_\Sigma = -\sum_n T\, \ln(1 + \exp(-\zeta_n/T))\,. \tag{5}
$$

In equation (4) ln denotes the principal branch of the logarithm, $f(\omega) = 1/(\exp(\omega/T) + 1)$ is the Fermi function, and C is a contour in the complex ω plane enclosing the first-order poles of the Fermi function in counterclockwise direction. In step (a) the transformation $\boldsymbol{U}(\omega)$ is performed under the trace. Convergence of the integral for $\omega \to \pm\infty$ is ensured by the Fermi function and by the factor $e^{\omega 0^+}$, respectively. Step (b) results from analytical continuation to real frequencies. In step (c) $-(1/\pi)\mathrm{Im}\, g_k(\omega + i0^+) \geq 0$ has been used (see Appendix B). At this point the causality of the Green's function is essential, as discussed above. In step (d) the Fermi function is written as a derivative with respect to ω and integration by parts is performed. Step (e) uses the results of Appendix C for the derivative of the step function. As the different diagonal elements of the Green's function, $g_k(\omega)$, have the same set of poles and zeros[1], the sum over k becomes trivial and yields a factor $2L$ only where L is the dimension of the hopping matrix, i.e. the number of orbitals. The factor 2 accounts for the two spin directions. The contribution from the poles of the self-energy (Appendix C) is denoted by R_Σ. Apart from this correction term, $\mathrm{Tr} \ln(-(\boldsymbol{G}_0(\boldsymbol{t})^{-1} - \boldsymbol{\Sigma}(\boldsymbol{t}'))^{-1})$ turns out to be the grand potential of a system of *non-interacting* quasiparticles with *unit* weight and energies given by the poles of $\boldsymbol{G}(\omega) \equiv (\boldsymbol{G}_0^{-1}(\omega) - \boldsymbol{\Sigma}(\omega))^{-1}$.

[1] We formally allow for poles of $g_k(\omega)$ and $\eta_k(\omega)$ with vanishing residue. Note that adding a pole with zero weight to $g_k(\omega)$ can only be accomplished if simultaneously a pole with zero weight is added to $\eta_k(\omega)$, and $\mathrm{Tr} \ln(-\boldsymbol{G})$ is unchanged.

Consider now the third term on the r.h.s. of equation (3). A calculation completely analogous to equation (4) results in:

$$T\sum_{\omega} e^{i\omega 0^+}\mathrm{tr}'\,\ln(-\boldsymbol{G}'(i\omega)) = \\ -2L\sum_{m} T\,\ln(1+\exp(-\omega'_m/T)) - R_{\Sigma}\,. \quad (6)$$

Here ω'_m are the poles of $\boldsymbol{G}'$. Again, the first term in equation (6) is the grand potential of a non-interacting system of fermions with one-particle energies given by the poles of the Green's function $\boldsymbol{G}'$. The same holds for the second term, but with energies given by the poles of the self-energy. By construction, the self-energy is the same for both, the original system and the reference system. Hence, the same correction term R_{Σ} appears in equations (4) and (6) and cancels out in equation (3).

Note that a pole of $\boldsymbol{G}(\omega)$ at $\omega=\omega_m$ with residue $\boldsymbol{R}_m \to 0$ implies a pole of $\boldsymbol{G}'(\omega)$ at the same frequency ω_m (with residue $\boldsymbol{R}'_m \to 0$). Hence, contributions due to poles with vanishing residues cancel out in equation (3). The reason is the following: Suppose that $g_k(\omega)=R_{k,m}/(\omega-\omega_m)$ for ω close to ω_m with residue $R_{k,m}\to 0$. For the diagonal elements of $\boldsymbol{t}+\boldsymbol{\Sigma}(\omega)$ this implies that $\eta_k(\omega)=(1/R_{k,m})(\omega-\omega_m)$ near ω_m. A zero of $\eta_k(\omega)$ with infinite positive coefficient $1/R_{k,m}$ must be due to $\boldsymbol{\Sigma}(\omega)$. Therefore, for the diagonal elements of $\boldsymbol{t}'+\boldsymbol{\Sigma}(\omega)$ this means that $\eta'_k(\omega)=(1/R_{k,m})(\omega-\omega_m)$. Consequently, $g'_k(\omega)\equiv 1/(\omega+\mu-\eta'_k(\omega))=R_{k,m}/(\omega-\omega_m)$ for ω close to ω_m with $R_{k,m}\to 0$. The argument also shows that although the residues do not appear in equations (4) and (6) explicitly, one can state that poles with small residues will give a small contribution in equation (3).

Based on the causality of the respective Green's functions, an efficient algorithm can be set up to find ω_m and ω'_m numerically which are then needed in equations (4) and (6). The poles of $\boldsymbol{G}'(\omega)$ are directly obtained from the diagonalization of the reference system. The problem consists in finding the poles of $\boldsymbol{G}(\omega)$. Allowing for poles with vanishing (very small) residue, one can assume the function $g'_k(\omega)$ for fixed but arbitrary k to display all the poles of $\boldsymbol{G}'(\omega)$. Since $g'_k(\omega)$ is of the form $g'_k(\omega)=\sum_m R'_{k,m}/(\omega-\omega'_m)$ with $R'_{k,m}\geq 0$, it is monotonically decreasing. Hence, there is exactly one zero of $g'_k(\omega)$ located in the interval between two adjacent poles ω'_m and ω'_{m+1}. As $g'_k(\omega)$ is monotonous, the zero ζ_m can easily be found numerically by an iterative bisection procedure. The zeros of $g'_k(\omega)$ are the poles of $\eta'_k(\omega)$ and the poles of $\eta'_k(\omega)$ are the same as the poles of $\eta_k(\omega)$. Now, since $g_k(\omega)=1/(\omega+\mu-\eta_k(\omega))$, $g_k(\omega)$ and $g'_k(\omega)$ must have the same set of zeros. The function $g_k(\omega)$ is monotonically decreasing. Therefore, the poles of $g_k(\omega)$ can be found between the ζ_m by using the same iterative bisection procedure once again.

4 Local approximations

In the following we consider H to be the single-band Hubbard model:

$$H=\sum_{ij\sigma} t_{ij}c^{\dagger}_{i\sigma}c_{j\sigma}+\frac{U}{2}\sum_{i\sigma} n_{i\sigma}n_{i-\sigma}\,. \quad (7)$$

For the reference system H' shown in Figure 1, the self-energy is local: $\Sigma_{ij}(\omega)=\delta_{ij}\Sigma(\omega)$. Clearly, the approximation is the better the more degrees of freedom are included in H'. The optimal local approximation is obtained with the most flexible (but local) trial self-energy. This is the DMFT which is recovered for an infinite number of uncorrelated bath sites (per original correlated site), i.e. for $n_{\mathrm{s}}-1\to\infty$. On the other hand, $n_{\mathrm{s}}=1$ corresponds to a Hubbard-I-type approximation. Here it will be shown that, for arbitrary n_{s}, the evaluation of the self-energy functional reduces to a one-dimensional integration only. This is an important simplification for any practical numerical (or even analytical) calculations.

In case that the self-energy is local it is advantageous to start from step (c) in equation (4). Assuming translational symmetry, the matrix $\boldsymbol{t}+\boldsymbol{\Sigma}(\omega)$ is diagonalized by Fourier transformation to reciprocal space. Its eigenvalues $\eta_k(\omega)$ are given by $\eta_k(\omega)=\epsilon(\boldsymbol{k})+\Sigma(\omega)$ where $k=(\boldsymbol{k},\sigma)$ and $\epsilon(\boldsymbol{k})$ is the tight-binding Bloch dispersion. The self-energy is taken to be spin-independent and independent of the site index, i.e. a paramagnetic homogeneous phase is assumed for simplicity. The second term on the r.h.s. of equation (3) then becomes:

$$\begin{aligned}&\mathrm{Tr}\ln(-(\boldsymbol{G}_0(\boldsymbol{t})^{-1}-\boldsymbol{\Sigma}(\boldsymbol{t}'))^{-1})\\ &\overset{(c)}{=}-\sum_{\boldsymbol{k}\sigma}\int d\omega\, f(\omega)\,\Theta\left(\omega+\mu-\epsilon(\boldsymbol{k})-\Sigma(\omega)\right)\\ &=-2L\int d\omega\, f(\omega)\int dz\,\rho_0(z)\,\Theta\left(\omega+\mu-z-\Sigma(\omega)\right)\\ &=2L\int d\omega\, f(\omega)\int dz\,R_0(z)\,\frac{d}{dz}\Theta\left(\omega+\mu-z-\Sigma(\omega)\right)\\ &=-2L\int d\omega\, f(\omega)\,R_0(\omega+\mu-\Sigma(\omega))\,. \end{aligned} \quad (8)$$

Here L is the number of lattice sites, the factor 2 stems for the spin summation, $\rho_0(z)=L^{-1}\sum_{\boldsymbol{k}}\delta(z-\epsilon(\boldsymbol{k}))$ is the non-interacting density of states, and $R_0(z)=\int_{-\infty}^{z}dz'\rho_0(z')$ is an antiderivative. Note that there is no "correction term" R_{Σ}, as the derivative in equation (8) is with respect to z.

The reference system H' is a set of decoupled single-impurity Anderson models with one correlated ("impurity") site and $n_{\mathrm{s}}-1$ bath sites each. The Hamiltonian is $H'=\sum_i H'(i)$ with

$$H'(i)=\sum_{\sigma}\epsilon_1 c^{\dagger}_{i\sigma}c_{i\sigma}+\frac{U}{2}\sum_{\sigma}n_{i\sigma}n_{i-\sigma} \\ +\sum_{\sigma,k=2}^{n_{\mathrm{s}}}\epsilon_k a^{\dagger}_{ik\sigma}a_{ik\sigma}+\sum_{\sigma,k}\left(V_k c^{\dagger}_{i\sigma}a_{ik\sigma}+\mathrm{h.c.}\right)\,. \quad (9)$$

The parameters ϵ_1, ϵ_k, and V_k for $k = 2, ..., n_s$ are the on-site energies of the impurity site and of the bath sites, and the hybridization between them, respectively. These are the variational parameters of the theory.

The third term on the r.h.s. of equation (3) reads:

$$\begin{aligned}&\mathrm{Tr}\ln(-(\boldsymbol{G}_0'(\boldsymbol{t}')^{-1} - \boldsymbol{\Sigma}(\boldsymbol{t}'))^{-1}) \\ &= 2LT\sum_{\omega} e^{i\omega 0^+}\left(\ln(-G_1'(i\omega)) + \sum_{k=2}^{n_s}\ln(-G_k'(i\omega))\right) \\ &= -2L\int_{-\infty}^{\infty} d\omega\ f(\omega)\left(\Theta(G_1'(\omega)) + \sum_{k=2}^{n_s}\Theta(G_k'(\omega))\right)\end{aligned} \tag{10}$$

where the first equation is derived in Appendix D and

$$G_1'(\omega) = \frac{1}{\omega + \mu - \epsilon_1 - \Delta(\omega) - \Sigma(\omega)} \tag{11}$$

is the impurity Green's function,

$$G_k'(\omega) = \frac{1}{\omega + \mu - \epsilon_k} \tag{12}$$

is the (free) conduction-band Green's function, and

$$\Delta(\omega) = \sum_{k=2}^{n_s}\frac{V_k^2}{\omega + \mu - \epsilon_k} \tag{13}$$

is the hybridization function. The final expressions (8) and (10) involve one-dimensional integrations only and can therefore be calculated numerically without serious problems.

5 Two-site dynamical impurity approximation

In the following we will focus on the case $n_s = 2$, i.e. on the two-site dynamical-impurity approximation ($n_s = 2$-DIA). There are different intentions which are followed up:

(i) For any approximation within the context of the SFA, one has to compute the self-energy of the reference system H'. As the interaction part is the same for both, H and H', this still constitutes a non-trivial many-body problem which can only be treated by numerical means in most cases. The reference system characterized by $N_c = 1$ and $n_s = 2$, represents an exception: For a special point in the space of model parameters (zero temperature, half-filling and $U = U_c$, the critical interaction for the Mott transition), the entire calculation can be done *analytically*. This not only includes the diagonalization of the reference system which actually is a simple dimer model but also and more important here, the exact evaluation of the self-energy functional for the trial self-energies considered and the subsequent variational optimization. Therefore, the study of the $n_s = 2$-DIA is ideally suited to elucidate different technical points which are relevant for any N_c and n_s and which must be considered carefully.

(ii) The $n_s = 2$-DIA must be considered as *inferior* when compared to approximations with higher n_s and when compared to $n_s = \infty$ (the DMFT) in particular. On the other hand, one has to keep in mind that the DMFT must always be supplemented by an additional (numerical) method to solve the mean-field equations which necessarily involves additional approximations. Even if the additional approximations can be controlled, DMFT results always depend on the accuracy of the numerical method employed. As concerns the $n_s = 2$-DIA, there is no such difficulty: The theory rests on a *single* approximation only, namely the restriction of the space $\mathcal{S}$ to self-energies representable by the two-site reference system – the rest of the calculation is rigorous. It is this conceptual simplicity which makes the approximation attractive.

(iii) That an approach referring to an $n_s = 2$-site SIAM is able to give reasonable results has been shown beforehand by the linearized DMFT (L-DMFT) [38–42]. The L-DMFT is a well-motivated but ad-hoc simplification of the full DMFT and maps the Hubbard model self-consistently onto the $n_s = 2$-site SIAM just at the critical point for the Mott transition. The L-DMFT can be also be considered to represent the lowest-order realization of a more general projective self-consistent method (PSCM) [22]. As compared to the full DMFT, the linearized theory yields surprisingly good estimates for the critical interaction U_c in the single-band model, on translation invariant lattices [38] as well as for lattice geometries with reduced translational symmetry [39]. The approach can also be extended beyond the critical regime [43]. The main disadvantage of the L-DMFT is that it not consistently derived from a thermodynamical potential. Another intention of the present paper is therefore to suggest a two-site method that conceptually improves upon the L-DMFT in this respect. In fact, as the parameters of the effective $n_s = 2$-site impurity model are determined via a physically meaningful variational principle, the two-site approximation within the SFA should be regarded as an *optimal* two-site approach. The interesting question is, of course, whether or not this improvement of the method also implies improved results. To this end the results from the analytical evaluation of the $n_s = 2$-DIA have to be compared with those of the L-DMFT and with available numerical results for $n_s = \infty$ (full DMFT). This represents a good check of the practicability of the new method. As the $n_s = 2$-site DIA still represents a very handy method, it can also be employed to investigate overall trends. It will be interesting to study the critical interaction U_c for a variety of different geometries (i.e. for different free densities of states).

Let us first consider a numerical evaluation of the theory. Figure 2 shows the results of a numerical calculation along the lines discussed above for the paramagnetic phase of the Hubbard model at half-filling and zero temperature. The free density of states (DOS) $\rho_0(z)$ is taken to be semi-elliptical with a band width $W = 4$. The calculations are performed using the $n_s = 2$-DIA, i.e. there is one bath site (per correlated site) only. Due to manifest particle-hole symmetry, two of the variational

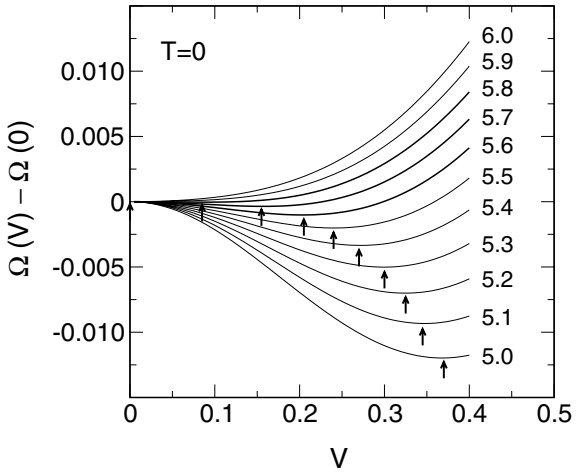

Fig. 2. The grand potential Ω (per site) as calculated from equation (3) and equations (8) and (10) for the reference system with $n_{\rm s} = 2$ as a function of the hybridization strength V (only the difference $\Omega(V) - \Omega(V = 0)$ is plotted). Calculations for the Hubbard model at zero temperature $T = 0$ and half-filling ($\mu = U/2$). The free density of states is taken to be semi-elliptical with a band width $W = 4$. The interaction strength is varied from $U = 5$ to $U = 6$ as indicated. Arrows indicate stationary points of the self-energy functional. The Mott transition takes place at a critical interaction strength $U_{\rm c} \approx 5.85$.

parameters, the on-site energies, are already fixed: $\epsilon_1 = 0$ and $\epsilon_2 = \mu = U/2$. As a function of the remaining variational parameter, the hybridization strength $V \equiv V_{k=2}$, the grand potential $\Omega(V) = \Omega[\boldsymbol{\Sigma}(V)]$ shows two (non-equivalent) stationary points for $U = 5$ (see Fig. 2): a minimum at a finite $V = 0.37$ and a maximum at $V = 0$ (as $\Omega(V) = \Omega(-V)$, there is another minimum at $V = -0.37$ which can be ignored here). The two stationary points correspond to two physically different phases: For $V > 0$ the interacting local density of states is finite at $\omega = 0$ while it vanishes for $V = 0$. So there is a metallic and an insulating phase coexisting. Due to the lower Ω at the respective stationary point, the metallic phase is stable as compared to the insulating one. With increasing U the optimal $V_{\rm met}$ and the energy difference $|\Omega(V_{\rm met}) - \Omega(0)|$ decrease. For $U = U_{\rm c} \approx 5.85$ there is a metal-insulator (Mott-Hubbard) transition which is characterized by a coalescence of the stable metallic with the metastable insulating phase. For $U > U_{\rm c}$ there is the insulating phase only.

Qualitatively, this continuous transition is completely consistent with the preformed-gap scenario [11,22] (however, see also Refs. [47–49]). For $U < U_{\rm c}$ the self-energy is a two-pole function. This leads to a three-peak structure in the interacting local density of states: Similar as in the full DMFT, there are two Hubbard "bands" separated by an energy of the order of U, and a quasi-particle resonance at $\omega = 0$. On approaching the critical interaction $U_{\rm c}$ from below, the weight z of the resonance vanishes linearly $z \sim (U_{\rm c} - U)$ leaving a finite gap for $U > U_{\rm c}$. As shown in reference [30] the quasi-particle weight calculated from the self-energy at the respective optimal $V = V_{\rm met}$ is in a very good quantitative agreement with results from full DMFT calculations in the whole range from $U = 0$ to $U = U_{\rm c}$ – for $n_{\rm s} = 4$ and even for $n_{\rm s} = 2$ which is the case considered here.

6 "Linearized" dynamical impurity approximation

In the following we will concentrate on the critical regime $U \to U_{\rm c}$. It will be shown that the critical interaction strength can be calculated analytically for $n_{\rm s} = 2$. The independent analytical result can be compared with the numerical one of the preceding section. This represents a strong test of the numerics.

Consider the function $\Omega(V) = \Omega[\boldsymbol{\Sigma}(V)]$. As $\Omega(V) = \Omega(-V)$ there must be a stationary point of $\Omega(V)$ at $V = 0$ for any U. This implies that the linear term in an expansion around $V = 0$ is missing, i.e.:

$$\Omega(V) = \Omega(0) + A \cdot V^2 + \mathcal{O}(V^4)\,. \tag{14}$$

The coefficient A depends on U. Assuming that the metal is stable against the insulator for $U < U_{\rm c}$, we must have $A < 0$ for $U < U_{\rm c}$ and $A > 0$ for $U > U_{\rm c}$. This is a necessary condition for a continuous ("second-order") transition and consistent with the numerical results displayed in Figure 2. Therefore, the critical point for the Mott transition within the two-site model is characterized by

$$A = 0\,. \tag{15}$$

The task is to calculate the three contributions to the grand potential following equation (3), to expand in V up the the second-order term and to find the interaction strength satisfying the condition (15).

Consider the grand potential of the reference system first. With $\epsilon_1 = 0$, $\epsilon_2 = U/2$ and $\mu = U/2$ the ground state of the two-site system, equation (9), lies is the invariant subspace with total particle number $N' = 2$. The ground-state energy E_0' is readily calculated:

$$E_0' = \frac{3}{4}U - \frac{1}{4}\sqrt{U^2 + 64V^2}\,. \tag{16}$$

At $T = 0$ the grand potential of the reference system is $\Omega' = LE_0' - L\mu\langle N'\rangle$. Therefore,

$$\Omega'/L = -\frac{U}{4} - \frac{1}{4}\sqrt{U^2 + 64V^2} = -\frac{U}{2} - \frac{8V^2}{U} + \mathcal{O}(V^4)\,. \tag{17}$$

Actually, this is the grand potential *per site*.

We proceed with the third term on the r.h.s. of equation (3). For the analytical calculation, it is convenient to start from equation (6):

$$T\sum_{\omega} \mathrm{tr}'\ \ln(-\boldsymbol{G}'(i\omega)) = 2L\sum_{r} \omega_r'\Theta(-\omega_r') - R_\Sigma \tag{18}$$

where it has been used that $-T\ \ln(1 + \exp(-\omega/T)) = \omega\Theta(-\omega)$ for $T = 0$. The factor 2 is due to the spin degeneracy. R_Σ will cancel out later. The Green's function

of the two-site model is easily calculated. There are four excitation energies, labeled by r, given by the four poles of the impurity Green's function at:

$$\omega_r' = \pm\frac{1}{4}\left(\sqrt{U^2+64V^2} \pm \sqrt{U^2+16V^2}\right) . \quad (19)$$

This yields:

$$T\sum_\omega \mathrm{tr}'\ \ln(-\boldsymbol{G}'(i\omega))/L = -U - \frac{32V^2}{U} + \mathcal{O}(V^4) - R_\Sigma/L\,. \quad (20)$$

Finally, for the second term on the r.h.s. of equation (3) we have:

$$T\sum_\omega \mathrm{tr}\ \ln(-\boldsymbol{G}(i\omega)) = 2L\sum_r \int_{-\infty}^{\infty} dz\ \rho_0(z)\,\omega_r(z)\Theta(-\omega_r(z)) - R_\Sigma\,. \quad (21)$$

Here, equation (4) has been used with $k = (\boldsymbol{k}, \sigma)$, and the $\boldsymbol{k}$ sum has been replaced by an integration over z weighted by the free DOS $\rho_0(z)$. For a given $z = \epsilon(\boldsymbol{k})$, the quasiparticle energies are obtained as the poles of the lattice Green's function in reciprocal space, i.e. from the solutions $\omega = \omega_r(z)$ of the equation $\omega+\mu-z-\Sigma(\omega) = 0$. To find the roots, the self-energy of the reference system is needed:

$$\Sigma(\omega) = \frac{U}{2} + \frac{U^2}{8}\left(\frac{1}{\omega-3V} + \frac{1}{\omega+3V}\right) . \quad (22)$$

This leads to a cubic equation:

$$\omega^3 - z\omega^2 - (9V^2 + U^2/4)\omega + 9zV^2 = 0\,. \quad (23)$$

The solutions for $V = 0$ are easily obtained. For small $V \neq 0$ we find one root near $\omega = 0$:

$$\omega_1(z) = \frac{36z}{U^2}\,V^2 + \mathcal{O}(V^4)\,, \quad (24)$$

and another one near $\omega = -U/2$:

$$\omega_2(z) = \frac{z}{2} - \frac{1}{2}\sqrt{z^2+U^2} - \left(\frac{18z}{U^2} + \frac{18}{U^2}\frac{z^2+U^2/2}{\sqrt{z^2+U^2}}\right)V^2 + \mathcal{O}(V^4)\,. \quad (25)$$

Because of the step function in equation (21), the third root near $\omega = U/2$ is not needed here. This yields:

$$T\sum_\omega \mathrm{tr}\ \ln(-\boldsymbol{G}(i\omega))/L = -R_\Sigma/L + 2\int_{-\infty}^{\infty} dz\ \rho_0(z)\ \left(\Theta(z)\frac{36z}{U^2}\,V^2 + \omega_2(z)\right) + \mathcal{O}(V^4)\,. \quad (26)$$

Inserting the results, equations (17, 20), and (26), into equation (3) and using the symmetry $\rho_0(z) = \rho_0(-z)$, we find:

$$\Omega/L = \mathrm{const.} + V^2\left(\frac{24}{U} + \frac{72}{U^2}\int_{-\infty}^{0} dz\ \rho_0(z)\,z - \frac{36}{U^2}\int_{-\infty}^{\infty} dz\ \rho_0(z)\frac{z^2+U^2/2}{\sqrt{z^2+U^2}}\right) + \mathcal{O}(V^4)\,. \quad (27)$$

Now, the condition (15) gives the critical U for the Mott transition:

$$U_\mathrm{c} = -3\int_{-\infty}^{0} dz\rho_0(z)z + \frac{3}{2}\int_{-\infty}^{\infty} dz\rho_0(z)\frac{z^2+U_\mathrm{c}^2/2}{\sqrt{z^2+U_\mathrm{c}^2}}. \quad (28)$$

This implicit analytical equation for U_c is the final result. For an arbitrary free DOS no further simplifications are possible.

7 Discussion

It should be stressed once more that equation (28) results from an exact variational principle simply by the restriction that the trial self-energies be representable by the two-site reference system. The two-site model generally yields a two-pole self-energy which is the minimal requirement for a three-peak structure of the single-particle excitation spectrum. Therefore, it may also be stated that equation (28) gives the optimal result for a two-pole self-energy.

Equation (28) turns out to be more complicated as compared to the result of the linearized DMFT [38]:

$$U_\mathrm{c}^{(\mathrm{L-DMFT})} = 6\sqrt{\int_{-\infty}^{\infty} dz\ \rho_0(z)\,z^2}\,. \quad (29)$$

Interestingly, the first term on the r.h.s. of equation (28) resembles Brinkman and Rice (Gutzwiller) result [50] for the critical interaction:

$$U_\mathrm{c}^{(\mathrm{BR})} = -16\int_{-\infty}^{0} dz\ \rho_0(z)\,z\,. \quad (30)$$

A rough approximation of the second term in (28) using $(z^2+U_\mathrm{c}^2/2)/\sqrt{z^2+U_\mathrm{c}^2} \to U_\mathrm{c}/2$ then yields $U_\mathrm{c} \approx 3U_\mathrm{c}^{(\mathrm{BR})}/4$. This reduction of the critical interaction as compared to the BR result is the dominating effect.

For a semi-elliptical free DOS with variance $\Delta = 1$ (band width $W = 4$), one has $U_\mathrm{c}^{(\mathrm{L-DMFT})} = 6$ and $U_\mathrm{c}^{(\mathrm{BR})} = 6.7906$. The numerical solution of equation (28) is straightforward and yields $U_\mathrm{c} = 5.8450$. As expected this is fully consistent with the numerical determination of U_c (Sect. 5). The result is close to the one predicted by the L-DMFT. Compared to numerical estimates from full DMFT calculations $U_\mathrm{c}^{(\mathrm{DMFT})} = 5.84$ (NRG, Ref. [23]) and

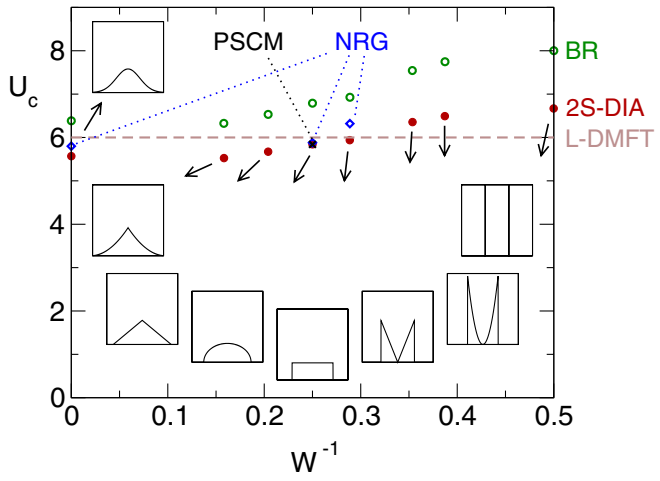

Fig. 3. Critical interaction U_c as a function of the inverse band width W^{-1}. Calculations for different (normalized) free densities of states $\rho_0(z)$ as indicated (where $-3 < z < 3$ and $0 < \rho_0(z) < 1.5$ in the insets).

Table 1. Critical interaction U_c as obtained from the SFA within the $n_s = 2$ dynamical impurity approximation for different free densities of states. Each DOS is normalized, $\int_{-\infty}^{\infty} \rho_0(z) = 1$, symmetric, $\rho_0(z) = \rho_0(-z)$, and has unit variance, $\Delta = \int_{-\infty}^{\infty} z^2 \rho_0(z) = 1$. $A(z) = \Theta(W/2 + z)\Theta(W/2 - z)$ is a cutoff function. W is the band width. The critical interaction from the Gutzwiller (Brinkman-Rice) approach [50] and the available full DMFT results are shown for comparison. The linearized DMFT [38] yields $U_c^{(\mathrm{L-DMFT})} = 6$ for any DOS with unit variance.

$\rho_0(z)$	W	$U_c^{n_s=2}$	U_c^{BR}	U_c^{DMFT}
Gaussian	∞	5.5663	6.3831	5.80[a]
$3A(z)(\lvert z\rvert - \sqrt{10})^2/20\sqrt{10}$	$2\sqrt{10}$	5.5284	6.3246	
triangle	$2\sqrt{6}$	5.6696	6.5320	
semi-ellipse	4	5.8450	6.7906	5.84[b], 5.88[a]
rectangle	$2\sqrt{3}$	5.9385	6.9282	6.32[c]
$A(z)\lvert z\rvert/2$	$2\sqrt{2}$	6.3554	7.5425	
$9\sqrt{3}A(z)z^2/10\sqrt{5}$	$2\sqrt{5/3}$	6.4944	7.7460	
$\delta(z-1)/2 + \delta(z+1)/2$	2	6.6686	8.0000	

[a] Ref. [23].
[b] Ref. [22].
[c] R. Bulla, private communication.

$U_c^{(\mathrm{DMFT})} = 5.88$ (PSCM, Ref. [22]), one can state that the prediction of the L-DMFT is improved.

Results for different free densities of states are displayed in Figure 3 and Table 1. For a meaningful comparison, each DOS has unit variance $\Delta = 1$ where $\Delta^2 = \int_{-\infty}^{\infty} dz \rho_0(z) z^2$. The band width W varies. The DOS with the smallest W (but $\Delta = 1$) consists of two δ-peaks while $W = \infty$ for a Gaussian DOS. Clearly, there is no true Mott transition in the former case (but also in the latter this is questionable). However, the inclusion of these extreme cases is instructive when studying the trend of U_c as a function of W. Note that for $\Delta = 1$ the L-DMFT yields $U_c = 6$ irrespective of the form of the DOS.

The critical interaction from the two-site DIA is always close the L-DMFT result but considerably lower than the Gutzwiller value. The two-site DIA confirms the central prediction of the L-DMFT that it is the variance of the DOS that is crucial for the critical interaction. However, there is also a weak trend superimposed, namely a systematic increase of U_c with decreasing band width W (with the exception of the Gaussian DOS). This is the same trend that is also present in the Gutzwiller results. It would be interesting to see whether or not this trend is confirmed by full DMFT calculations. Comparing the full DMFT results for the Gaussian, for the rectangular and the semi-elliptic DOS shows the mentioned trend. However, the comparison of the two-site DIA and of the L-DMFT with the full DMFT for the available numerical data is not fully conclusive.

8 Finite temperatures

So far only the zero-temperature limit has been considered. The Mott transition at finite temperatures, however, is particularly interesting as there is a comprehensive physical picture available with a comparatively complex phase diagram. This phase diagram in the U-T plane was first suggested by the iterative perturbation theory [9,11]. The nature of the transition and the topology of the phase diagram have been established entirely using analytic arguments [49] and has been worked out quantitatively using different numerical methods [24,27–29]. The critical regime is accessible by the projective self-consistent method [22].

As this phase diagram represents a valuable benchmark for any approximation, it is interesting to see whether or not it can be rederived within the most simple two-site DIA. The application of the theory for finite T is straightforward but can no longer be done analytically. As for the derivation of the $T = 0$ results in the non-critical regime (see Sect. 5), calculations are performed along the lines of Section 4.

It turns out that for finite temperatures the Mott transition is predicted to be discontinuous. This is demonstrated in Figure 4 which shows $\Omega(V)$ for different T and fixed $U = 5.2$ ($n_s = 2$). At low but finite T there are three stationary points (see arrows) corresponding to three different phases of the system. The metallic phase has the largest value $V = V_{\mathrm{met}}$. With increasing temperature V_{met} decreases and $\Omega(V_{\mathrm{met}}) \propto T^2$ for low T. This gives a linear entropy $S(T) = -\partial\Omega(T)/\partial T$ and a linear specific heat $C_v = T\partial S(T)/\partial T = \gamma T \propto z^{-1}T$ as it is characteristic for a Fermi liquid ($\mu = U/2$ is fixed). The insulating phase has the smallest value $V = V_{\mathrm{ins}}$, and the grand potential $\Omega(V_{\mathrm{ins}}) \propto T$ for low T. For $T \to 0$ the entropy approaches $S \to L \ln 2$ reflecting a 2^L-fold ground-state degeneracy of the insulator which is known to be an artifact of mean-field theory [11]. The specific heat C_v vanishes exponentially for $T \to 0$. For $U = 5.2$ and low T, however, the insulating phase is metastable as compared to the metallic

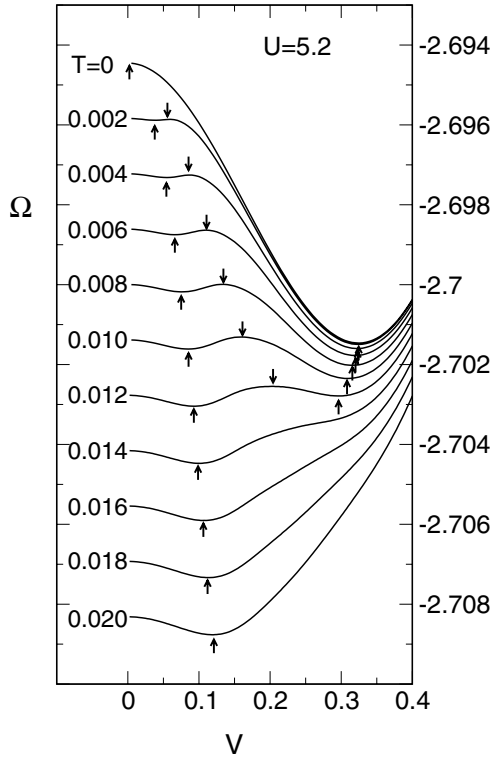

Fig. 4. Grand potential per site at $U = 5.2$ for different T as a function of V. The arrows indicate the stationary points.

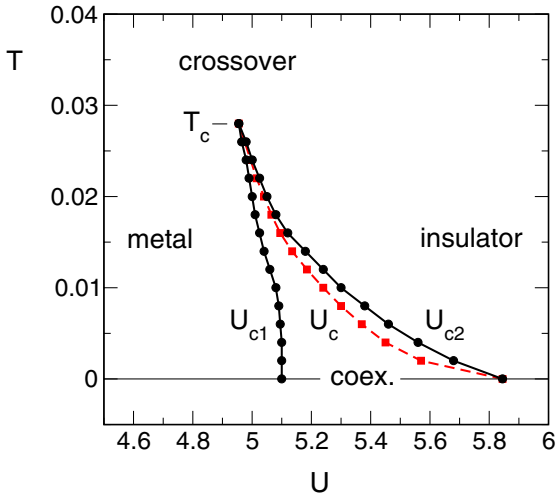

Fig. 5. Phase diagram for the Mott transition in the paramagnetic phase of the Hubbard model at half-filling. Calculations for a semi-elliptical density of states with band width $W = 4$. Reference system H': two-site model. U_{c2}: critical interaction strength up to which there is a (metallic) solution smoothly connected with the metal at $U = 0$. U_{c1}: critical interaction strength down to which there is an (insulating) solution smoothly connected with the Mott insulator for $U \to \infty$. U_c: first-order transition line in the coexistence region, terminating at the second-order critical point at T_c.

phase since $\Omega(V_{\rm ins}) > \Omega(V_{\rm met})$. Due to the different behavior at low T, there must be a temperature $T_c(U)$ where $\Omega(V_{\rm ins}) = \Omega(V_{\rm met})$. In fact, for $T = 0.012 > T_c(U = 5.2)$ the insulator is stable as compared to the metal. At $T_c(U)$ or, conversely, at a critical interaction $U_c(T)$, the $n_{\rm s} = 2$-DIA thus predicts a first-order transition with a discontinuous jump in the entropy. As can be seen in Figure 4, the metallic phase ceases to exist for still higher temperatures, and only the insulating phase is left. This is due to a coalescence of the metallic with a third phase at another critical temperature $T_{c2}(U)$ (or, conversely, at a critical interaction $U_{c2}(T)$). This third phase turns out to be less stable as compared to the metal and to the insulator in the entire parameter regime. Similarly, one can define a critical temperature $T_{c1}(U)$ (at smaller U) and thus a critical interaction $U_{c1}(T)$ where the insulating phase coalesces with the third phase.

Calculations for different U and T have been performed to obtain the entire phase diagram within the two-site approach. The result is shown in Figure 5. For $U \leq U_{c2}(T)$ there is a metallic phase which is smoothly connected to the $U = 0$ limit. On the other hand, for $U \geq U_{c1}(T)$ there is an insulating phase which is smoothly connected with the Mott insulator for $U \to \infty$. Metallic and insulating phase are coexisting for $U_{c1}(T) \leq U \leq U_{c2}(T)$. At zero temperature, the metal is stable as compared to the insulator in the entire coexistence region, and the transition is continuous at $U_c = U_{c2}$. For finite temperatures the transition is discontinuous at a critical interaction $U_c(T)$ with $U_{c1}(T) \leq U_c(T) \leq U_{c2}(T)$. With increasing temperatures the coexistence region $U_{c1}(T) \leq U \leq U_{c2}(T)$ shrinks and disappears above a critical temperature T_c which is defined via $U_{c1}(T_c) = U_{c2}(T_c)$. Above T_c the metallic phase is smoothly connected with the insulating phase.

Qualitatively, this is exactly the same result that is obtained within the full DMFT [11]. It is very remarkable that the rather complex topology of the phase diagram can be reproduced with a comparatively simple two-site model as a reference system. This shows that it is essential to perform the mapping onto the reference system in a way which is thermodynamically consistent and which is controlled by a physical variational principle. Note that the L-DMFT, or its extension away from the critical point at $T = 0$ [43], fails to reproduce the discontinuous transition for $T > 0$ and the critical temperature T_c due to the ad-hoc character of the approximation.

Quantitatively, one should expect some deviations from the results of the full DMFT due to the simplicity of the two-site model. Comparing with the NRG result [24] for $U_{c1}(T = 0) \approx 4.8 - 5.0$, the two-site approximation overestimates the critical interaction by a few per cent. The determination of the critical temperature is difficult in any numerical approach. $T_c \approx 0.05 - 0.08$ is estimated from the QMC and NRG results of references [24,27]. Thus, the two-site approximation underestimates T_c by more than a factor 2. It is worth mentioning that the numerical effort to obtain the entire phase diagram in the $U - T$ plane is of the order of a few minutes on a standard workstation which is negligible as compared to a DMFT-QMC calculation.

9 Conclusions

Our present understanding of the Mott-Hubbard transition is mainly based on the exact solution of the one-dimensional case on the one hand and on the $D = \infty$ mean-field picture provided by the DMFT on the other hand. For the physically more relevant two- or three-dimensional Hubbard model, however, neither the analytical concepts developed for $D = 1$ nor the mean-field theory can be expected to give an essentially correct and comprehensive description. Direct numerical approaches, such as QMC, are able to give essentially exact results for a $D = 2, 3$ dimensional lattice of finite spatial extent. However, the relevance of the results for the thermodynamic limit and, in many cases, for the low-temperature, low-energy regime remains an open question.

In this situation, a combination of a direct numerical approach for systems of finite size with the mean-field concept appears to be advantageous. This is more or less the direction that is followed up by the different cluster extensions of the DMFT [37,51–53]. Via a generalized mean-field concept, the original lattice problem given by the Hamiltonian H is mapped onto a cluster problem described by a Hamiltonian H'. In fact, due to the presence of strong short-range antiferromagnetic correlations a considerable revision of the mean-field picture is probably necessary [54]. However, the cluster extensions of the DMFT suffer from the fact that the mean-field formulation requires that the sites of the finite cluster are coupled to uncorrelated baths with an infinite number of degrees of freedom each. This circumstance complicates the practical solution of the H' problem (which must be solved repeatedly during the self-consistency cycle) so much that additional approximations are required and/or stochastic numerical methods.

The self-energy-functional approach offers an interesting alternative as the reference system H', the original model H is mapped onto, is by no means completely predetermined. The SFA gives a very general prescription how this mapping can be performed while keeping the thermodynamical consistency of the approach as an explicit expression for the grand potential is provided. In this way the DMFT and the cellular DMFT are recovered as certain limits for special choices of H', namely for a decoupled system of clusters of size $N_\mathrm{c} = 1$ or $N_\mathrm{c} > 1$ including couplings to $n_\mathrm{b} = \infty$ bath degrees of freedom. There is, however, the additional possibility to construct approximations with $n_\mathrm{b} < \infty$ which are consistent in themselves in the same way as are the DMFT and the C-DMFT.

Now, the question is whether or not an approximation with a finite number of bath sites $n_\mathrm{b} < \infty$ can be tolerated. Note that even in the (C-)DMFT it becomes necessary to reduce the problem posed by H' with $n_\mathrm{b} = \infty$ to a numerically tractable one with a *finite* number of degrees of freedom. While this additional approximation is controlled within QMC or ED approaches, for example, it nevertheless violates thermodynamical consistency. Within the SFA, on the contrary, the approximation is derived from a thermodynamical potential for any n_b, infinite or finite or even so small as $n_\mathrm{b} = 1$. Depending on the quantity and accuracy one is interested in, there can be a rapid convergence with respect to n_b (cf. Ref. [30]) so that a small number might be sufficient. For cluster approximations, the best choice is by no means clear as it must be balanced with the choice of the cluster size N_c. This strongly depends on the lattice dimension. In fact, it has been shown [32] that for the one-dimensional Hubbard model a larger N_c is to be preferred as compared to a larger n_b.

In this context, it is interesting to see where one are led to with the most simple reference system conceivable. This is a model H' characterized by $N_\mathrm{c} = 1$ and $n_\mathrm{b} = 1$ which yields the so-called two-site dynamical impurity approximation (DIA). The answer is given with the present paper: Even in this approximation the Mott transition shows up. At zero temperature the transition turns out to be continuous at a finite critical interaction U_c where there is a coalescence of the metallic with a coexisting insulating phase. For finite temperatures, on the other hand, the transition is discontinuous. The first-order line $U_c(T)$ terminates at a second-order critical point $(U_c(T_c), T_c)$, and for $T > T_c$ there is a smooth crossover only. This is qualitatively the same picture that has been found beforehand in the full DMFT. Furthermore, the two-site DIA yields a U_c at $T = 0$ that is surprisingly close to the result of the full DMFT. In this respect the two-site DIA is of similar quality as the linearized DMFT [38], another approach that is based on a mapping onto the two-site SIAM. Whether or not the U_c-results of the two-site DIA improve on those of the L-DMFT is difficult to decide in view of the existing (full) DMFT data. More important, however, the conceptual improvement gained is substantial: While the mapping procedure on the two-site model, though physically motivated, is done in an ad-hoc way in the L-DMFT, the two-site DIA is derivable from a thermodynamical potential and can be characterized as an optimal two-site approach in fact.

The fact that a reasonable mean-field description of the Mott transition is possible even for the simple two-site DIA, motivates further SFA studies of the transition with improved approximations in the future (e.g. using finite clusters, $N_\mathrm{c} > 1$, and small n_b). In case of larger and more complex reference systems, however, it becomes more and more important to have a numerically efficient and accurate method for the evaluation of the self-energy functional at hand. The detailed analysis of the different contributions to the functional has been another major intention of the present study. Using the causality properties of the Green function, it has been shown that the important $\mathrm{Tr}\ln(-\boldsymbol{G})$ term can be written as the grand potential of a system of non-interacting quasi-particles with unit weight (apart from a correction term that cancels out in the functional eventually). While this result is also interesting by itself, it is very well suited for an efficient numerical implementation. As the energies of the fictitious quasi-particles are given by the poles of the Green function, they can be found in a comparatively simple way by exploiting general causality properties. In particular, there is no need for a small but finite Lorentzian broadening,

$\omega \to \omega + i\delta$, which must be introduced in a more direct way to evaluate the functional [32,33]. This will become important when studying the critical regime of the Mott transition, where an accurate computation of small energy differences is vital, using an approximation with several variational parameters. Studies in this direction are intended for the future.

It is a pleasure to acknowledge valuable discussions with B. Michaelis, E. Arrigoni and W. Hanke. This work is supported by the Deutsche Forschungsgemeinschaft (SFB 290 "Metallische dünne Filme: Struktur, Magnetismus und elektronische Eigenschaften" and SFB 410 "II-VI-Halbleiter: Wachstumsmechanismen, niederdimensionale Strukturen und Grenzflächen").

Appendix A

Here is will be shown that the Green's function $\boldsymbol{G}$ is causal: For any $\boldsymbol{t'}$ the self-energy $\boldsymbol{\Sigma} = \boldsymbol{\Sigma}(\boldsymbol{t'})$ is causal since it is defined to be the exact self-energy of the reference system $H' = H_0(\boldsymbol{t'}) + H_1(\boldsymbol{U})$. Likewise, the Green's function $\boldsymbol{G}_0$ is causal. It has to be shown that $\boldsymbol{G} \equiv (\boldsymbol{G}_0^{-1} - \boldsymbol{\Sigma})^{-1}$ is causal if $\boldsymbol{\Sigma}$ and the free Green's function $\boldsymbol{G}_0$ are known to be causal.

Causality of $\boldsymbol{G}$ means (i) that $G_{\alpha\beta}(\omega)$ is analytic in the entire complex ω plane except for the real axis and (ii) that $\boldsymbol{G}_{\rm ret}(\omega) = \boldsymbol{G}(\omega + i0^+) = \boldsymbol{G}_{\rm R} - i\boldsymbol{G}_{\rm I}$ for real ω with $\boldsymbol{G}_{\rm R}$, $\boldsymbol{G}_{\rm I}$ Hermitian and $\boldsymbol{G}_{\rm I}$ positive definite. (i) is easily verified. To show (ii) we need the following

Lemma: For Hermitian matrices $\boldsymbol{A}$, $\boldsymbol{B}$ with $\boldsymbol{B}$ positive definite, one has

$$\frac{1}{\boldsymbol{A} \pm i\boldsymbol{B}} = \boldsymbol{X} \mp i\boldsymbol{Y} \tag{A.1}$$

with $\boldsymbol{X}$, $\boldsymbol{Y}$ Hermitian and $\boldsymbol{Y}$ positive definite. The *proof* of the Lemma is straightforward:

$$\frac{1}{\boldsymbol{A} \pm i\boldsymbol{B}} = \boldsymbol{B}^{-\frac{1}{2}} \frac{1}{\boldsymbol{B}^{-\frac{1}{2}}\boldsymbol{A}\boldsymbol{B}^{-\frac{1}{2}} \pm i} \boldsymbol{B}^{-\frac{1}{2}} = \boldsymbol{D} \frac{1}{\boldsymbol{C} \pm i} \boldsymbol{D} \tag{A.2}$$

with $\boldsymbol{C}$, $\boldsymbol{D}$ Hermitian and $\boldsymbol{D} = \boldsymbol{B}^{-\frac{1}{2}}$ positive definite. Let $\boldsymbol{C} = \boldsymbol{U}\boldsymbol{c}\boldsymbol{U}^\dagger$ with $\boldsymbol{U}$ unitary and $\boldsymbol{c}$ diagonal. Then

$$\frac{1}{\boldsymbol{A} \pm i\boldsymbol{B}} = \boldsymbol{D}\boldsymbol{U} \frac{1}{\boldsymbol{c} \pm i} \boldsymbol{U}^\dagger \boldsymbol{D} = \boldsymbol{D}\boldsymbol{U} \frac{\boldsymbol{c} \mp i}{\boldsymbol{c}^2 + 1} \boldsymbol{U}^\dagger \boldsymbol{D} = \boldsymbol{X} \mp i\boldsymbol{Y} \tag{A.3}$$

with $\boldsymbol{X}$ Hermitian and

$$\boldsymbol{Y} = \boldsymbol{D}\boldsymbol{U} \frac{1}{\boldsymbol{c}^2 + 1} \boldsymbol{U}^\dagger \boldsymbol{D} \tag{A.4}$$

Hermitian and positive definite.

Consider a fixed (real) frequency ω. Since $\boldsymbol{G}_0$ is causal, $\boldsymbol{G}_{0,\rm ret} = \boldsymbol{G}_{0,\rm R} - i\boldsymbol{G}_{0,\rm I}$ with $\boldsymbol{G}_{0,\rm R}$, $\boldsymbol{G}_{0,\rm I}$ Hermitian and $\boldsymbol{G}_{0,\rm I}$ positive definite. Using the lemma, $\boldsymbol{G}_{0,\rm ret}^{-1} = \boldsymbol{P}_{\rm R} + i\boldsymbol{P}_{\rm I}$ with $\boldsymbol{P}_{\rm R}$, $\boldsymbol{P}_{\rm I}$ Hermitian and $\boldsymbol{P}_{\rm I}$ positive definite. Since $\boldsymbol{\Sigma}$ is causal, $\boldsymbol{\Sigma}_{\rm ret} = \boldsymbol{\Sigma}_{\rm R} - i\boldsymbol{\Sigma}_{\rm I}$ with $\boldsymbol{\Sigma}_{\rm R}$, $\boldsymbol{\Sigma}_{\rm I}$ Hermitian and $\boldsymbol{\Sigma}_{\rm I}$ positive definite. Therefore,

$$\boldsymbol{G}_{\rm ret} = \frac{1}{\boldsymbol{P}_{\rm R} + i\boldsymbol{P}_{\rm I} - \boldsymbol{\Sigma}_{\rm R} + i\boldsymbol{\Sigma}_{\rm I}} = \frac{1}{\boldsymbol{Q}_{\rm R} + i\boldsymbol{Q}_{\rm I}} \tag{A.5}$$

with $\boldsymbol{Q}_{\rm R}$ Hermitian and $\boldsymbol{Q}_{\rm I}$ Hermitian and positive definite. Using the lemma once more, shows $\boldsymbol{G}$ to be causal.

Appendix B

Consider the function

$$f(\omega) = \sum_m \frac{R_m}{\omega - \omega_m} \tag{B.1}$$

with real isolated first-order poles at $\omega = \omega_m$ and positive residues $R_m > 0$. We have:

$$-\frac{1}{\pi}{\rm Im} f(\omega + i0^+) > 0 \tag{B.2}$$

In Section 3 $f(\omega) = g_k(\omega) = 1/(\omega + \mu - \eta_k(\omega))$.

In a polar representation $-f(\omega + i0^+) = r(\omega)e^{i\phi(\omega)}$ with $-\pi < \phi(\omega) \leq \pi$. On the principal branch of the logarithm and for real ω one has ${\rm Im}\ln(-f(\omega + i0^+)) = \phi(\omega)$. For any $\omega \neq \omega_m$ we have ${\rm Im}(-f(\omega + i0^+)) = 0^+$ from equations (B.1) and (B.2) and thus $\phi(\omega) = \pi$ for $-f(\omega) < 0$, and $\phi(\omega) = 0$ for $-f(\omega) > 0$. Consequently,

$${\rm Im}\ln(-f(\omega + i0^+)) = \pi\,\Theta(f(\omega)) = \pi\,\Theta(1/f(\omega))\,, \tag{B.3}$$

where Θ is the step function. For $\omega = \omega_m$, the imaginary part of $-f(\omega + i0^+)$ diverges. However, $-\pi < \phi(\omega) \leq \pi$ (in fact $\phi(\omega_m + 0^+) = -\pi/2$ and $\phi(\omega_m - 0^+) = \pi/2$). Hence, Im $\ln(-f(\omega + i0^+))$ remains finite at $\omega = \omega_m$ and can be ignored in an integration over real ω as the poles of $f(\omega)$ are isolated.

Appendix C

Consider a function $f = f(\omega)$ which is analytical except for isolated first-order poles on the real axis and which is real for real ω. $\Theta(f(\omega))$ is constant almost everywhere, and thus the derivative $d\Theta(f(\omega))/d\omega$ vanishes almost everywhere. A non-zero derivative may either occur if $f(\omega) = 0$, i.e. at the zeros ω_m. This gives a contribution:

$$\delta(f(\omega))f'(\omega) = \sum_m \frac{f'(\omega_m)}{|f'(\omega_m)|}\delta(\omega - \omega_m) \tag{C.1}$$

where $f'(\omega) \equiv df(\omega)/d\omega$. A second contribution arises from the first-order poles of $f(\omega)$ at ζ_n. The poles are the zeros of the function $1/f(\omega)$. Note that $\Theta(f(\omega)) = \Theta(1/f(\omega))$ since the sign of the argument is unchanged. Thus the contribution due to the poles is:

$$\delta(1/f(\omega))(1/f)'(\omega) = \sum_n \frac{(1/f)'(\zeta_n)}{|(1/f)'(\zeta_n)|}\delta(\omega - \zeta_n). \tag{C.2}$$

We have:

$$\frac{d\Theta(f(\omega))}{d\omega} = \delta(f(\omega))f'(\omega) + \delta(1/f(\omega))(1/f)'(\omega) = \sum_m^{\{\text{zeros}\}} \epsilon_m \delta(\omega-\omega_m) + \sum_n^{\{\text{poles}\}} \epsilon_n \delta(\omega-\zeta_n) \tag{C.3}$$

with $\epsilon_m = \pm 1$ and $\epsilon_n = \pm 1$ depending on the sign of the slope of f at the zeros ω_m and the sign of the residue of f at the poles ζ_n, respectively.

Consider the function $f(\omega) = \omega + \mu - \eta_k(\omega)$. The zeros of f are the poles of the diagonalized Green's function $1/(\omega+\mu-\eta_k(\omega))$ which has positive residues. This implies a positive f' at ω_m and $\epsilon_m = +1$. The poles of f are the poles of the self-energy which has positive residues. Thus the residues of f at the poles are negative and $(1/f)'$ is negative at ζ_n and $\epsilon_n = -1$. Hence:

$$\frac{d}{d\omega}\Theta(\omega+\mu-\eta_k(\omega)) = \sum_m \delta(\omega-\omega_m) - \sum_n \delta(\omega-\zeta_n)\,. \tag{C.4}$$

Appendix D

The reference system H' is a set of decoupled single-impurity Anderson models with one-particle energy of the impurity site ϵ_1, conduction-band energies ϵ_k with $k = 2, ..., n_{\rm s}$ and hybridization strengths V_k. We first calculate the eigenvalues of the hopping matrix $\boldsymbol{t}'$. The matrix is block diagonal with respect to the site index i. Each block is labeled by the "orbital" index $k = 1, ..., n_{\rm s}$. There are non-zero elements of the matrix for $k = 1$, $k' = 1$, and $k = k'$ only:

$$t'_{kk'} = (1-\delta_{k1})\delta_{k'1}\, V_k + \delta_{k1}(1-\delta_{k'1})\, V_{k'} + \delta_{kk'}\, \epsilon_{k'} \tag{D.1}$$

Furthermore, $\Sigma_{kk'}(\omega) = \delta_{k1}\delta_{k'1}\Sigma(\omega)$. Using

$$\det \begin{pmatrix} d_1 & a_2^* & a_3^* & a_4^* & ... \\ a_2 & d_2 & 0 & 0 & ... \\ a_3 & 0 & d_3 & 0 & ... \\ a_4 & 0 & 0 & d_4 & ... \\ ... & ... & ... & ... & ... \end{pmatrix} = \det \begin{pmatrix} \widetilde{d}_1 & 0 & 0 & 0 & ... \\ 0 & d_2 & 0 & 0 & ... \\ 0 & 0 & d_3 & 0 & ... \\ 0 & 0 & 0 & d_4 & ... \\ ... & ... & ... & ... & ... \end{pmatrix} \tag{D.2}$$

where $\widetilde{d}_1 = d_1 - \sum_{k=2}^{n_{\rm s}} |a_k|^2/d_k$ and the general relation $\mathrm{tr}\ln \boldsymbol{A} = \ln\det \boldsymbol{A}$, we find:

$$\begin{aligned} \frac{1}{2}\mathrm{tr}'\ln(-\boldsymbol{G}'(i\omega)) &= \ln\det \frac{-1}{i\omega+\mu-\boldsymbol{t}'-\boldsymbol{\Sigma}(i\omega)} \\ &= \ln\det \begin{pmatrix} -G'_1 & 0 & 0 & ... \\ 0 & -G'_2 & 0 & ... \\ 0 & 0 & -G'_3 & ... \\ ... & ... & ... & ... \end{pmatrix} \\ &= \ln(-G_1(i\omega)) + \sum_{k=2}^{n_{\rm s}} \ln\left(-G_k(i\omega)\right) \end{aligned} \tag{D.3}$$

with $G_1(i\omega)$ and $G_k(i\omega)$ for $k = 2, ..., n_{\rm s}$ as defined by equations (11, 12). The factor 1/2 accounts for the two spin directions.

References

1. M. Imada, A. Fujimori, Y. Tokura, Rev. Mod. Phys. **68**, 13 (1998)
2. F. Gebhard, *The Mott Metal-Insulator Transition* (Springer, Berlin, 1997)
3. N.F. Mott, *Metal-Insulator Transitions* (Taylor and Francis, London, 1990), 2nd edn.
4. J. Hubbard, Proc. R. Soc. London A **276**, 238 (1963)
5. M.C. Gutzwiller, Phys. Rev. Lett. **10**, 159 (1963)
6. J. Kanamori, Prog. Theor. Phys. (Kyoto) **30**, 275 (1963)
7. J.M. Luttinger, J.C. Ward, Phys. Rev. **118**, 1417 (1960)
8. E. Dagotto, Rev. Mod. Phys. **66**, 763 (1994)
9. A. Georges, G. Kotliar, Phys. Rev. B **45**, 6479 (1992)
10. M. Jarrell, Phys. Rev. Lett. **69**, 168 (1992)
11. A. Georges, G. Kotliar, W. Krauth, M.J. Rozenberg, Rev. Mod. Phys. **68**, 13 (1996)
12. W. Metzner, D. Vollhardt, Phys. Rev. Lett. **62**, 324 (1989)
13. E. Müller-Hartmann, Int. J. Mod. Phys. B **3**, 2169 (1989)
14. U. Brandt, C. Mielsch, Z. Phys. B **75**, 365 (1989)
15. U. Brandt, C. Mielsch, Z. Phys. B **79**, 295 (1990)
16. A. Georges, W. Krauth, Phys. Rev. B **48**, 7167 (1993)
17. M.J. Rozenberg, G. Kotliar, X.Y. Zhang, Phys. Rev. B **49**, 10181 (1994)
18. M. Caffarel, W. Krauth, Phys. Rev. Lett. **72**, 1545 (1994)
19. M. Rozenberg, G. Moeller, G. Kotliar, Mod. Phys. Lett. B **8**, 535 (1994)
20. Q. Si, M.J. Rozenberg, G. Kotliar, A.E. Ruckenstein, Phys. Rev. Lett. **72**, 2761 (1994)
21. M.P. Eastwood, F. Gebhard, E. Kalinowski, S. Nishimoto, R.M. Noack, Eur. Phys. J. B **35**, 155 (2003), `cond-mat/0303085`
22. G. Moeller, Q. Si, G. Kotliar, M. Rozenberg, D.S. Fisher, Phys. Rev. Lett. **74**, 2082 (1995)
23. R. Bulla, Phys. Rev. Lett. **83**, 136 (1999)
24. R. Bulla, T.A. Costi, D. Vollhardt, Phys. Rev. B **64**, 045103 (2001)
25. J.E. Hirsch, R.M. Fye, Phys. Rev. Lett. **56**, 2521 (1986)
26. J. Schlipf, M. Jarrell, P.G.J. van Dongen, N. Blümer, S. Kehrein, T. Pruschke, D. Vollhardt, Phys. Rev. Lett. **82**, 4890 (1999)
27. M.J. Rozenberg, R. Chitra, G. Kotliar, Phys. Rev. Lett. **83**, 3498 (1999)
28. J. Joo, V. Oudovenko, Phys. Rev. B **64**, 193102 (2001)
29. N. Blümer, Ph.D. thesis, Universität Augsburg, 2002
30. M. Potthoff, Eur. Phys. J. B **32**, 429 (2003)
31. G. Baym, L.P. Kadanoff, Phys. Rev. **124**, 287 (1961)
32. M. Potthoff, M. Aichhorn, C. Dahnken, Phys. Rev. Lett. **91**, 206402 (2003)
33. C. Dahnken, M. Aichhorn, W. Hanke, E. Arrigoni, M. Potthoff, `cond-mat/0309407`
34. C. Gros, R. Valenti, Phys. Rev. B **48**, 418 (1993)
35. D. Sénéchal, D. Pérez, M. Pioro-Ladrière, Phys. Rev. Lett. **84**, 522 (2000)
36. M.G. Zacher, R. Eder, E. Arrigoni, W. Hanke, Phys. Rev. B **65**, 045109 (2002)
37. G. Kotliar, S.Y. Savrasov, G. Pálsson, G. Biroli, Phys. Rev. Lett. **87**, 186401 (2001)

38. R. Bulla, M. Potthoff, Eur. Phys. J. B **13**, 257 (2000)
39. M. Potthoff, W. Nolting, Phys. Rev. B **60**, 7834 (1999)
40. Y. Ōno, R. Bulla, A.C. Hewson, Eur. Phys. J. B **19**, 375 (2001)
41. Y. Ōno, R. Bulla, A.C. Hewson, M. Potthoff, Eur. Phys. J. B **22**, 283 (2001)
42. Y. Ōno, M. Potthoff, R. Bulla, Phys. Rev. B **67**, 035119 (2003)
43. M. Potthoff, Phys. Rev. B **64**, 165114 (2001)
44. E. Runge, E.K.U. Gross, Phys. Rev. Lett. **52**, 997 (1984)
45. R. Chitra, G. Kotliar, Phys. Rev. B **63**, 115110 (2001)
46. H.Q. Lin, J.E. Gubernatis, Comput. Phys. **7**, 400 (1993)
47. S. Kehrein, Phys. Rev. Lett. **81**, 3912 (1998)
48. R.M. Noack, F. Gebhard, Phys. Rev. Lett. **82**, 1915 (1999)
49. G. Kotliar, Eur. Phys. J. B **11**, 27 (1999)
50. W.F. Brinkman, T.M. Rice, Phys. Rev. B **2**, 4302 (1970)
51. A. Schiller, K. Ingersent, Phys. Rev. Lett. **75**, 113 (1995)
52. M.H. Hettler, A.N. Tahvildar-Zadeh, M. Jarrell, T. Pruschke, H.R. Krishnamurthy, Phys. Rev. B **58**, R7475 (1998)
53. A.I. Lichtenstein, M.I. Katsnelson, Phys. Rev. B **62**, R9283 (2000)
54. T. Maier, M. Jarrell, T. Pruschke, J. Keller, Eur. Phys. J. B **13**, 613 (2000)